Supporting Information

Lu et al. 10.1073/pnas.0908560106

SI Discussion

VBIM Vector Construction: Poly(A) Signal Mutation for Forward Orientation Promoter Placement. Due to the poly(A) signal within the U3/R junction of the MLV and HIV 3′ LTRs, which leads to the termination/polyadenylation of transcripts initiated from upstream promoters, outbound promoters aimed at altering transcription of neighboring genomic DNA can only be placed within the retroviral backbone in reverse orientation (Fig. S1*A*). However, a reverse orientation promoter drives transcription toward the 5′ LTR, leading to promoter interference that significantly decreases the number of full-length viral mRNA molecules that can be packaged, ultimately leading to low virus titers. To circumvent the low titers generated from the reverse orientation vectors, we proposed that removing the poly(A) signal from the integrated provirus would permit placement of the promoter in the forward orientation, and efficient read-through into neighboring sequences upon integration (Fig. S1*B*). Particularly helpful for this design is work performed in the Berkhout laboratory, where the secondary structure of the poly(A) signal-containing hairpin has been mutated to either stabilized or destabilized hairpin structures (1, 2).

Many of the reported poly(A) mutations reduced genomic RNA content within virions, suggesting a critical role for the hairpin structure in packaging and/or stability of virion RNA. Therefore, specifically deleting or mutating the consensus poly(A) signal without consideration of RNA hairpin secondary structure will have detrimental effects on viral production. However, one poly(A) mutant in particular, the E mutant, was created where a portion of the poly(A) hairpin was deleted, including the AAUAAA poly(A) signal, but a minimal hairpin structure was maintained with similar thermodynamic stability as the wild-type hairpin form. In the poly(A) "E mutant," deletion of the poly(A) signal alone was not detrimental to viral packaging, viral RNA content, reverse transcription or viral protein production, provided that an additional SV40 poly(A) signal was cloned downstream of the 3′ LTR to permit efficient polyadenylation of the viral RNA in packaging cells (2). We have recreated this E mutation in both the 5′ and 3′ LTR poly(A) signals of a standard lentiviral vector (pLV-GFP) and cloned an SV40 poly(A) signal downstream of the 3′ LTR. The mutant poly(A) vector backbone, which is described in detail below, will be referred to as pLV^{E}-GFP (Fig. S2*A*). Importantly, following infection with pLV^{E}-GFP, reverse transcription will eliminate the SV40 poly(A) signal (since it is downstream of the 3′ LTR), leaving a poly(A)-deficient provirus inserted into the genome and allowed transcriptional read-through to occur into neighboring genomic sequences (Fig. S2*B*). As reported earlier, this will result exclusively in read-through transcripts that depend upon a cellular poly(A) signal for proper mRNA processing (1, 2).

Testing pLV^{E}-GFP -GFP Readthrough. To test whether mutation of the poly(A) signal in the pLV^{E}-GFP vector would allow efficient viral production, infection and integration, 293T cells were transfected with lentiviral packaging constructs and pLV-GFP control or pLV^{E}-GFP vector. The resulting viruses were used to infect 293T or BJ fibroblasts. GFP expression was strong in both transfected populations, but surprisingly, cells infected with the pLV^{E}-GFP virus expressed a higher level of GFP protein relative to the control pLV-GFP (Fig. S2*C*), even though the viral titers and resulting infection efficiencies were nearly identical, as determined by GFP expression (Fig. S3). Since spliced mRNAs are more stable than unspliced messages, the increased intensity of GFP in cells infected with pLV^{E}-GFP is likely due to the splicing of viral/cellular fusion mRNAs (3).

To confirm that poly(A)-trapping was occurring, individual clones were picked and expanded from the 293T cells infected with pLV-GFP virus (as a control, two clones) and pLV^{E}-GFP virus (seven clones). RNA was subjected to RT-PCR analysis with a lentiviral specific 5′ primer and an anchored polyT 3′ primer (as depicted in Fig. S2*B*). Appropriate polyadenylation of a transcript produced from the pLV-GFP provirus would result in the amplification of a 250-base pair product using these primers. In contrast, the absence of a viral derived polyadenylation signal, which is expected from a pLV^{E}-GFP proviral integration, would lead to read-through such that an amplified product could only be obtained from a cellular poly(A) signal. This will result in varying lengths of the RT-PCR products, depending upon the insertion site distance from the cellular poly(A) signal.

In agreement with expectations, a single predominant product was produced from the RT-PCR analysis of the pLV-GFP control vector-infected cells, while numerous products of different sizes were observed in the pLV^{E}-GFP infected cells (Fig. S2*D*). The infection efficiency of pLV^{E}-GFP permits numerous integrations per cell as observed by the numerous RT-PCR products observed in each clone. In addition, these integrations represent a subset of the integrations since not all insertions will aquire a poly(A) signal leading to polyadenylation. These data suggest that the pLV^{E}-GFP vectors are packaged efficiently, infect cells as well as standard lentiviral vectors, and that the resulting integrations efficiently acquire cellular poly(A) signals necessary for processing and production of a properly functioning mRNA molecules.

Creating a Promoter Insertion Cassette. Having a lentiviral-based vector backbone capable of producing (1) high-titer virus to infect cells and (2) hybrid viral-cellular RNA fusion transcripts, the next consideration was the components needed to create and identify dominant changes in gene transcription. Herein, the components relating to the promoter, including transcription and RNA processing, are termed the "promoter insertion cassette." The cytomegalovirus (CMV) immediate early promoter is small (≈700 bp) and drives strong transgene expression, at least 10-fold higher than an MLV LTR, in many cell types. For the purpose of promoter-based insertional mutagenesis, we anticipate that the strongest level of expression will yield the greatest number of mutants and have chosen to use a CMV promoter.

To create a full-length CMV promoter that could also be regulated following selection for mutant phenotypes, a heptamerized tetracycline operator (TO) was cloned just upstream of the CMV promoter in pLV^{E}-GFP. The addition of the TO allows one to regulate the CMV promoters activity after mutants have been created, preventing the need for a cell line expressing the tetracycline-transactivator proteins (tTA). The TO provides no advantage or disadvantage to the activity of the full-length CMV promoter in the absence of a regulatory tetracycline operator-dependent repressor (4, 5). The cDNA encoding GFP was retained downstream of the CMV promoter to provide a method for determining viral titers in the supernatant collected from packaging cells and allow measurement of the desired number of integration events. The Woodchuck hepatitis virus posttranscriptional regulatory element (WPRE) was maintained to increase the fusion transcript stability and protein expression.

WPRE elements can increase protein expression by as much as 5 fold relative to messages lacking a WPRE (6). Finally, a FLAG epitope tag was embedded into an optimized adenoviral splice donor site (provided by R. Padgett, Cleveland Clinic Foundation) and placed downstream of the GFP and WPRE to facilitate splicing and fusion of the viral RNA with splice acceptors in the neighboring exons. Three different reading frames of the FLAG-SD were created so that each splice acceptor (SA) site in the genome could potentially produce a FLAG-fusion protein. To ensure that potential proteins encoded by the fusion message can be appropriately translated, an internal ribosome entry sequence (IRES) was included between the WPRE and the FLAG-SD. The finalized versions have been termed Validation-Based Insertional Mutagenesis vectors (VBIM vectors; Fig. 1*A*).

In addition to the forward orientation VBIM vectors shown in Fig. 1, a reverse orientation VBIM vector was also created and experimentally compared (Fig. S4*A*). As expected, the GFP expression was significantly impaired in the packaging cells, relative to the forward orientation vectors. The reduction in the amount of GFP mRNA produced from the VBIM-reverse implicates promoter interference between the 5′ LTR and the CMV promoter, resulting in a decrease in both viral mRNAs and GFP mRNAs and diminished infection efficiency (Fig. S4*B*).

SI Materials and Methods

VBIM Plasmid Construction. The pVBIM set of validation based insertional mutagenesis vectors was created using pLVR-GFP-LoxP (a kind gift from Dr. Peter Chumakov, Cleveland Clinic) as the lentiviral backbone, referred to as pLV-GFP. The "E mutation" was generated in the 5′ LTR by PCR amplification of the U5 and mutated R region using *Pfu* Turbo DNA polymerase (Stratagene) with the U5–1 forward primer 5′-AGAAAAAG-CACCGTGCATGCCGATTGG-3′ and the R-1 reverse primer 5′-AGAAAAAGCACCGTGCATGCCGATTGG-3′ using pLV-GFP as a template. Next, the mutated R region and U3 of the 5′ LTR was PCR amplified with the R-2 forward primer 5′-AGTGTGTGCCCGTCTGTTGTGTGA-3′ and U3–1 reverse primer 5′-CCGAATTTTTTCCCATCGCGATCTAAT-TCT-3′. A final PCR was done combining both products of the previous reactions and using the U5–1 and U3–1 primers. The mutated 5′ LTR was digested with *Sph*I and *Nru*I and cloned into pLV-GFP. To create the "E mutation" within the 3′ LTR, a similar strategy was used. The U5–2 forward primer: 5′-CTTCTGCGCTGAATGAGATCTGGTACCTTT-3′ and R-1 reverse primer were used to amplify the U5 and R regions within the 3′ LTR. The R-2 forward primer and U3–2 reverse primer 5′-TCTGGAATAGCTCAGAGGCCGAGGCGGCCT-3′ were used to amplify the R region and U3 of the 3′ LTR. The resulting products were combined and subjected to a final round of PCR amplification using the U5–2 and U3–2 primers. The mutated 3′ LTR was digested with *Kpn*I and *Sfi*I and cloned into pLV-GFP, containing the "E-mutation" in the 5′ LTR, resulting in the pLV^{E}-GFP described in *SI Text*. The tetracycline operator was cloned into pLV^{E}-GFP by PCR amplification, using a forward primer containing a *Cla*I site 5′-TATAATCGATTAC-CCGGGTCGAGAGTTCCGCGTTACATAA-3′ and a reverse primer containing a *Sma*I site 5′-CGATGACTAATACGTA-GATGTACTGCC-3′. The resulting PCR product was digested with ClaI and SmaI and cloned into pLV^{E}-GFP. The insertion of the IRES and adenoviral splice donor sequences was performed by PCR amplification of the IRES using a forward primer containing an *Xba*I site, 5′-TATATCTAGAAATTCCGC-CCCTCTCCCTCCCCCCCCCCTA-3′, and a reverse primer, 5′-GGAAGGTCGTCTCCTTGTGGGTTGTGGC-3′, using pIRES2Puro (Clontech) as a template. The adenoviral splice donor sequence was amplified by PCR using the forward primer: 5′-phospho GGGCGCGTTCGTCCTCACTCTCTTCCG-3′ and a reverse primer containing a *Kpn*I site, 5′- TAAAGG-TACCAGATCTCATTCAGCGCAGAAG-3′, using pADL (provided by Dr. Richard Padgett, The Cleveland Clinic). The PCR products were cut with *Xba*I and *Kpn*I and cloned into pLV^{E}-GFP. Finally, Kozak, ATG, and FLAG sequences in all three reading frames were introduced between the *Bam*HI and *Eco*RI sequences within the adenoviral splice donor. The oligonucleotides, 5′- GATCCACCATGGATTACAAGGAT-GACGACGATAAG-3′ with 5′- AATTCTTATCGTCGT-CATCCTTGTAATCCATGGTG-3′ were annealed and ligated into the *Bam*HI and *Eco*RI sites to create the first reading frame, pVBIM-SD1. The second and third reading frames were generated by annealing 5′- GATCCACCATGGATTACAAGGAT-GACGACGATAAG-3′ with 5′- AATTCTTATCGTCGT-CATCCTTGTAATCCATGGTG-3′ or 5′- GATCCACCAT-GGATTACAAGGATGACGACGATAAG-3′ and 5′-AATTCTTATCGTCGTCATCCTTGTAATCCATGGTG-3′ and ligating into the *Bam*HI and *Eco*RI sites of pVBIM, creating pVBIM-SD2 and pVBIM-SD3.

Transfections and Luciferase Assays. Constructs were transfected into cell lines by using the Lipofectamine Transfection Reagent and PLUS Reagent (Invitrogen Life Technologies) for either 48 or 72 h, as indicated in the descriptions of individual experiments. To establish stable pools, cells were co-transfected with a plasmid encoding a puromycin resistance gene, and selected in 1 μg/mL puromycin 48 h after transfection. For NFκB luciferase assays, the κB-luciferase construct p5XIP10 κB (with five tandem copies of the κB site from the IP10 gene), was transfected transiently into the cells and a β-galactosidase construct was co-transfected, to normalize the transfection efficiency. Transfections and luciferase assays were carried out essentially as described by Lu et al. (7).

EMSAs. The oligomer used for NFκB binding (5′-AGTT-GAGGGGACTTTCCCAGGC-3′, Santa Cruz Biotechnology), was labeled with [γ-^{32}P] ATP by the polynucleotide kinase method, following the protocol provided by Promega. Whole-cell lysates were prepared and analyzed essentially as described by Lu et al. (7).

1. Das AT, Klaver B, Klasens BI, van Wamel JL, Berkhout BA (1997) Conserved hairpin motif in the R-U5 region of the human immunodeficiency virus type 1 RNA genome is essential for replication. *J Virol* 71:2346–2356.
2. Klasens BI, Das AT, Berkhout B (1998) Inhibition of polyadenylation by stable RNA secondary structure. *Nucleic Acids Res* 26:1870–1876.
3. Nott A., Le HH, Moore MJ (2004) Splicing enhances translation in mammalian cells: an additional function of the exon junction complex. *Genes Dev* 18:210–222.
4. Wiznerowicz M, Trono D (2003) Conditional suppression of cellular genes: Lentivirus vector-mediated drug-inducible RNA interference. *J Virol* 77:8957–8961.
5. Deuschle U, Meyer WK, Thiesen HJ (1995) Tetracycline-reversible silencing of eukaryotic promoters. *Mol Cell Biol* 15:1907–1914.
6. Zufferey R, Donello JE, Trono D, Hope TJ (1999) Woodchuck hepatitis virus posttranscriptional regulatory element enhances expression of transgenes delivered by retroviral vectors. *J Virol* 73:2886–2892.
7. Lu T, Sathe SS, Swiatkowski SM, Hampole CV, Stark GR (2004) Secretion of cytokines and growth factors as a general cause of constitutive NFκB activation in cancer. *Oncogene* 23:2138–2145.

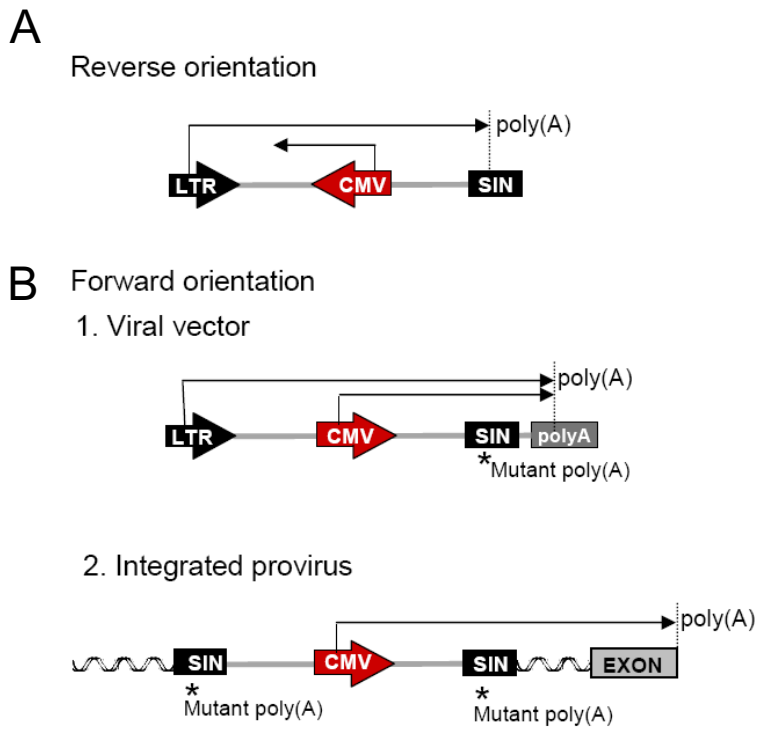

Fig. S1. Comparison of reverse and forward orientation insertional mutagenesis vectors. (*A*) Reverse orientation promoter insertion vectors are designed so that transcription from the mutagenic promoter (CMV, in this example) is driven away from the proviral poly(A) signal in the 3′ LTR. While this prevents polyadenylation following integration into the genome, this design results in transcriptional interference during virus packaging since the promoter activity of the 5′ LTR drives production of the viral mRNA. This interference during packaging significantly decreases viral titers. (*B*) Forward orientation promoter insertion vectors are designed with mutated poly(A) signals in the LTRs, so that transcription from the CMV promoter of an integrated provirus does not result in polyadenylation and does not interfere with the LTR during virus packaging. A poly(A) signal included downstream of the 3′ LTR results in appropriate viral mRNA polyadenylation for proper virus packaging, but is not included in the integrated provirus. This permits transcriptional ''read-through'' into neighboring genomic sequences, thus altering gene expression.

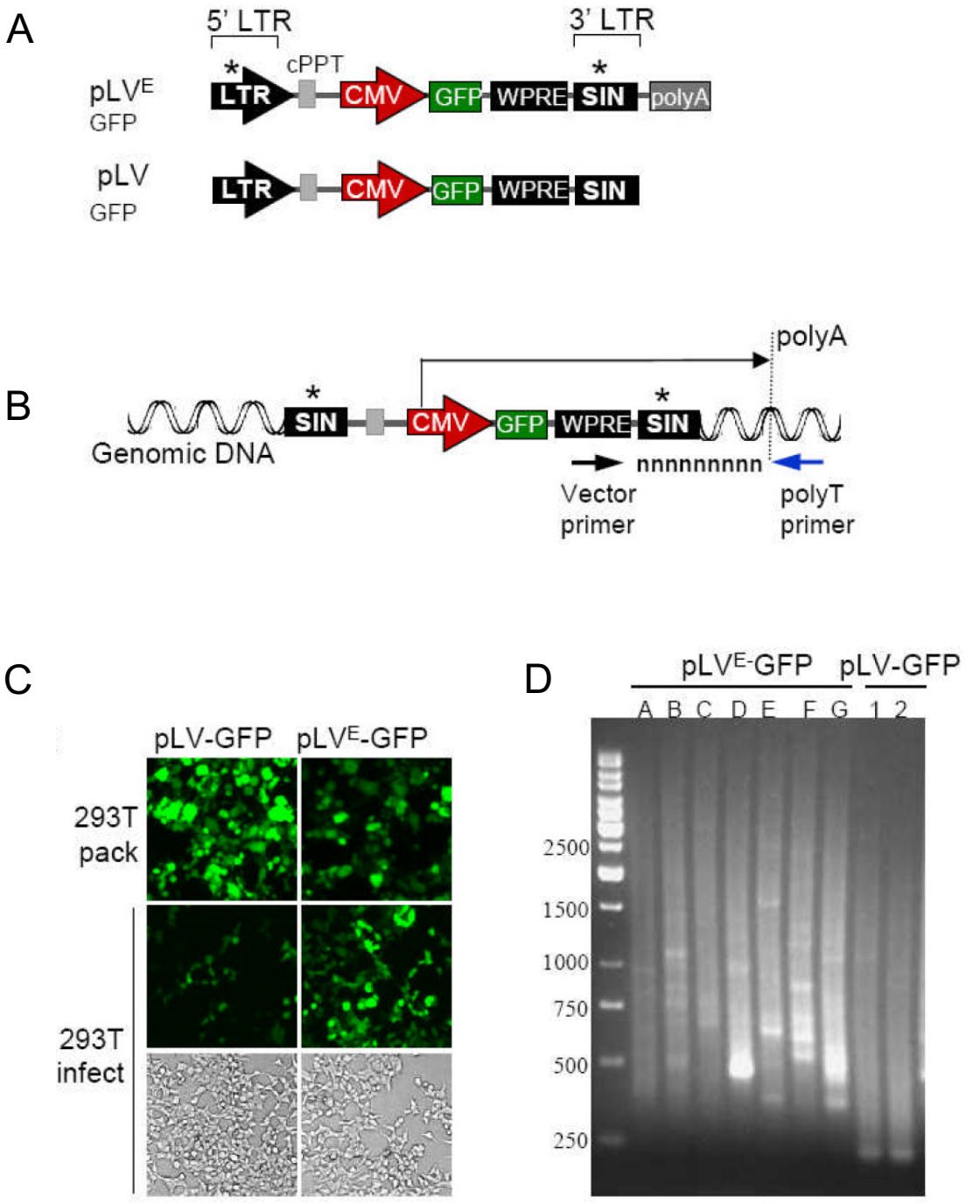

Fig. S2. Creating and testing polyA mutant HIV-based vectors. (*A*) Illustration of pLV-GFP control and pLV^{E}-GFP vector design, which has deletions of both the 5′ and 3′ poly(A) signal as described by Das et al. [poly(A) deletion denoted by the *]. (*B*) Illustration of a predicted pLV^{E}-GFP proviral integration within a coding region. (*C*) 293T cells were transfected with pLV-GFP or pLV^{E}-GFP and packaging constructs and examined for GFP expression by microscopy (293T pack). Viral supernatants were collected and used to infect 293T cells, and GFP expression was examined again (293T infect). All pictures were taken using the same exposure time for valid comparison. (*D*) RNA from individual 293T clones infected with pLV-GFP control or pLV^{E}-GFP was subjected to RT-PCR analysis using a vector specific 5′ primer (black, panel *B*) and an anchored polyT 3′ primer (blue, panel *B*). Polyadenylation from the pLV-GFP control proviral transcript should yield an approximately 250-bp product (lanes 1 and 2) while polyadenylation of a viral/cellular hybrid message will produce products that vary depending on the distance between the site of integration and the cellular polyA (lanes A–G).

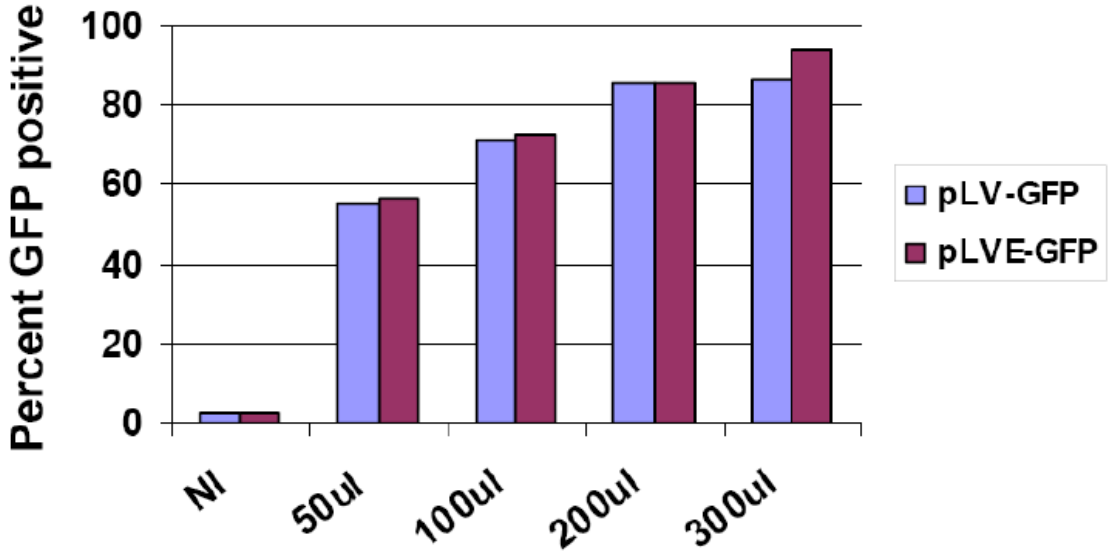

Fig. S3. High viral titers from the polyA-mutant pLV^{E}-GFP. 293T cells were transfected with pLV-GFP and a pLV^{E}-GFP vector containing a poly(A) deletion in both the 5′ and 3′ LTRs. Viral supernatants were collected and used to infect 293T cells, using the volume of viral supernatant shown in a total volume of 1.0 mL media in a 24-well plate. FACS analysis was used to quantify the percentage of cells that were GFP positive.

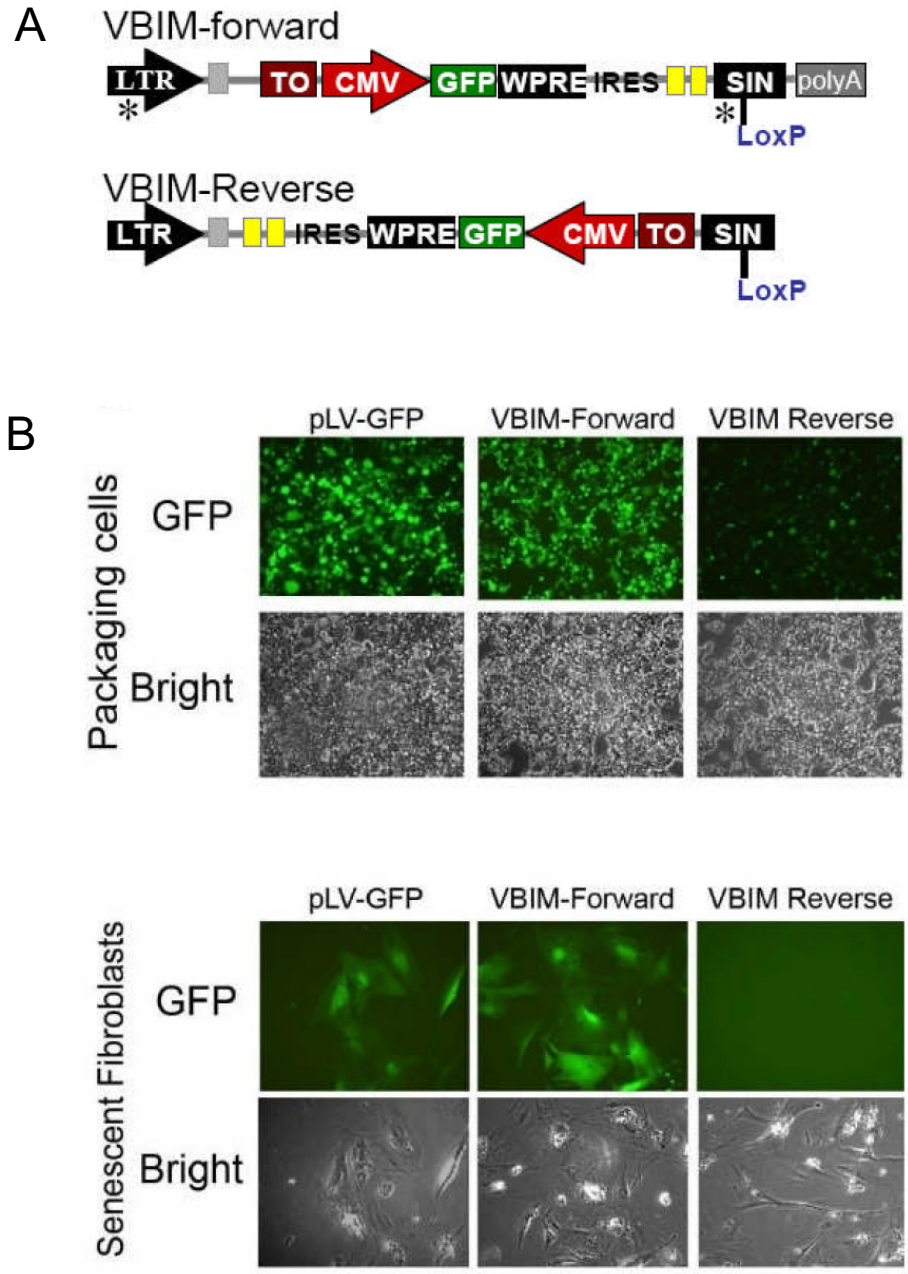

Fig. S4. Comparing VBIM forward and reverse orientation promoter insertion viruses. (*A*) The promoter insertion cassette (comprising TO-CMV-GFP-WPRE-IRES-FLAG/SD) was cloned in reverse orientation into pLV-GFP or in forward orientation in pLV^{E}-GFP. (*B*) 293T cells were transfected with each vector and packaging constructs and GFP expression was analyzed in both the packaging cells and infected senescent BJ fibroblasts to illustrate the increased efficiency achieved with the VBIM-forward viruses.

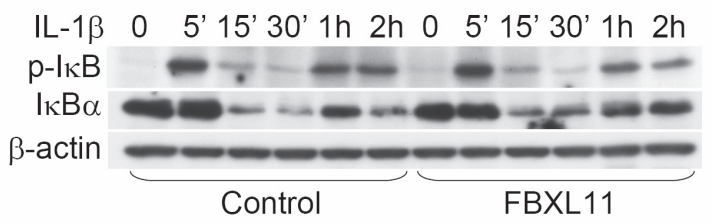

Fig. S5. Expression of FBXL11 does not affect phosphorylation and degradation of IκBα significantly. Western analysis, showing levels of phosphorylated and total IκBα in 293C6 cells and the same cells in which FBXL11 have been over-expressed, both treated with 10 ng/mL IL-1β.